XXI ICTAM, 15–21 August 2004, Warsaw, Poland

A STUDY OF PARTICLE DEBONDING WITH ANISOTROPY

Brian Nyvang Legarth
Department of Mechanical Engineering, Solid Mechanics, Technical University of Denmark

Summary Failure arising from debonding of rigid inclusions embedded in an elastic-viscoplastic matrix, modeled with plastic anisotropy, is investigated numerically using a plane strain biaxially loaded unit cell. Periodical boundary conditions are used to represent cases where the principal axes of anisotropy are inclined relative to the tensile direction. The average stress-strain response of the cell is evaluated and debonding is observed as a sudden stress drop. Depending on the initial orientation of the principal axes of plastic anisotropy, debonding in the present material is significantly delayed due to a reduction of the yield stress.

INTRODUCTION

Material properties like the Young modulus, the yield stress, the ductility and the fracture toughness are strongly affected by adding second phase particle to an otherwise pure material. Commonly, the fracture toughness is reduced due to void nucleation and growth along the particle-matrix interface. An early study of inclusion debonding was carried out in Ref. [1]. Besides the presence of inclusions, many parameters have a crucial impact on the strength of the composite, in particular the constitutive conditions of the matrix material and the inclusions, the bonding at the particle-matrix interface and the geometrical configuration of the composite.

PROBLEM FORMULATION AND MATERIAL DESCRIPTION

Here, focus is given to debonding of rigid inclusions of elliptical cross sections embedded in a plastically anisotropic matrix material using a unit cell model subjected to periodical boundary conditions. This allows for arbitrary initial orientation of the principal axes of plastic anisotropy. The periodical boundary conditions ensure compatibility as well as force equilibrium across any cell edge. The constitutive modeling of the matrix material is based on an multiplicative decomposition of the deformation gradients taking full account of small elastic and finite viscoplastic strains. The plastic strain increments are evaluated on the basis of a yield function, $J(\hat{\sigma}_{ij})$, where $\hat{\sigma}_{ij}$ are true stress components. In addition to the isotropic von Mises yield surface, this work considers two anisotropic yield criteria, namely Hill[2] and the proposal by Barlat *et al.*[3], subsequently referred as Hill-48 and Barlat-91. The hardening is isotropic. On compact form Hill-48 can be expressed as

$$J = \sqrt{\frac{3}{2(F+G+H)}\left[F(\hat{\sigma}_{22}-\hat{\sigma}_{33})^2 + G(\hat{\sigma}_{33}-\hat{\sigma}_{11})^2 + H(\hat{\sigma}_{11}-\hat{\sigma}_{22})^2 + 2N\hat{\sigma}_{12}^2 + 2L\hat{\sigma}_{23}^2 + 2M\hat{\sigma}_{13}^2\right]} \quad (1)$$

For $F = G = H = 1$ and $N = L = M = 3$ this yield function simplifies to the isotropic von Mises yield criterion. Barlat-91 can be expressed as

$$J = \left(\frac{\Phi}{2}\right)^{1/d} \quad \text{with} \quad \Phi = [S_1 - S_2]^d + [S_2 - S_3]^d + [S_1 - S_3]^d \quad (2)$$

where S_i are the principal values of a modified stress deviator, which includes six coefficients of anisotropy. The exponent d depends on the crystal structure, and is here taken to be eight corresponding to FCC-structures.
Debonding is modeled by the phenomenological cohesive zone model proposed by Tvergaard[4]. For increasing interfacial separation, the traction across the interface reaches a maximum, then decreases and eventually vanishes.

RESULTS AND DISCUSSION

The numerical results are obtained incrementally by applying a finite element method based on the principle of virtual work in an updated Lagrangian formulation using constant strain quadrilaterals elements. Due to highly unstable solution regimes and the periodical boundary conditions the combined finite element and Rayleigh-Ritz procedure developed by Tvergaard[5] is adopted. The results presented here are limited to circular inclusions in quadratic cells (volume fraction of 3%) loaded such that the average stress in the main tensile direction is haft the average stress in the transverse direction. Fig. 1 shows the calculated true stress versus logarithmic strain in the main tensile direction for plastically isotropic matrix material as well as plastically anisotropic matrix material using Barlat-91 for different values of the initial orientation of plastic anisotropy, θ_0. The sudden stress drop indicates the point of debonding initiation. The yield stress in plane strain tension for Hill-48 and Barlat-91 can be shown to vary periodically for any set of the coefficients of anisotropy, and has the same values at any of the four orientations $\pm\theta_0$ and $\pm(90^o - \theta_0)$. Minimum and maximum values are obtain for $\theta_0 = 45^o + 90^o z$ and $\theta_0 = 90^o z$ with $z = [.. -1, 0, 1..]$, respectively. This observation is recognized in Fig. 1 since the results for $\theta_0 = 0^o$ and $\theta_0 = 22.5^o$ coincide with the results for $\theta_0 = 90^o$ and $\theta_0 = 67.5^o$, respectively. For a high yield stress a large fraction of the critical interfacial stress will be generated in the elastic range and debonding will occur after a relatively small amount of deformation, as shown in Fig. 1 for $\theta_0 = 0^o$ and $\theta_0 = 90^o$. As the yield stress decreased, larger overall deformation is required in order to generate stresses near the inclusion that are high enough to initiate debonding. This effect is seen in Fig. 1 for $\theta_0 = 22.5^o, \theta_0 = 67.5^o$ and $\theta_0 = 45^o$.

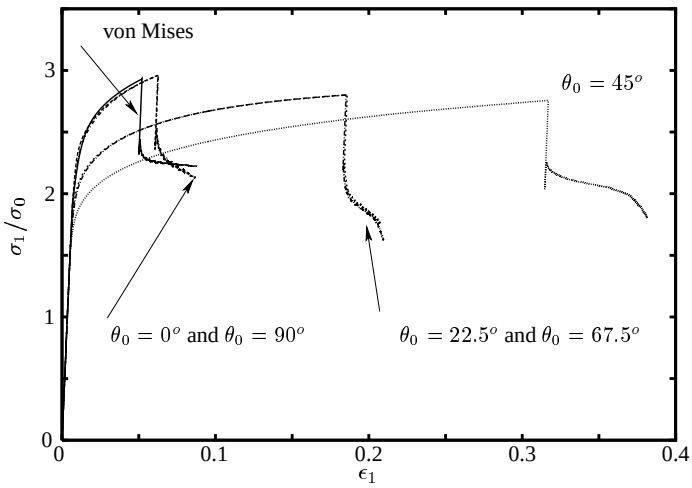

Figure 1: Stress strain responses for Barlat-91. The sudden stress drop indicates the point of debonding initiation.

For selected overall strains, ϵ_1, contours of constant effective plastic strain, ϵ^{p}, are shown in the deformed configuration in Fig. 2 using Hill-48 and Barlat-91 with $\theta_0 = 22.5^o$. For the configurations where debonding has occurred, $\epsilon_1 = 0.1$ or $\epsilon_1 = 0.2$, the contours illustrate intensive plastic deformation in the region near the void. Especially at the tip of the void where the inclusion is still bonded, high gradients of the effective plastic strain are found, indicating progressive void growth due to further debonding. Wavy deformation of the initially straight cell edges is observed due to development of non-symmetric shear stress across the cell boundaries.

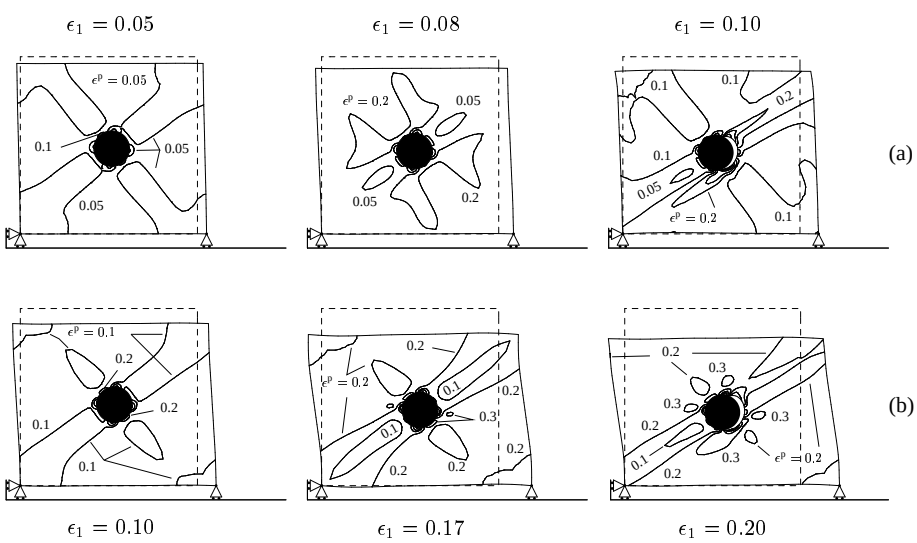

Figure 2: Deformed configurations for $\theta_0 = 22.5^o$ at different overall strains. The undeformed geometry is shown by the dashed line. (a) Hill-48 (b) Barlat-91.

For elliptical cross sections of the inclusion or for non-quadratic cells anisotropy due to the geometry is induced in addition to the plastic anisotropy. Results based on combinations of these two types of anisotropy will be shown as well.

ACKNOWLEDGMENT

This work is supported by The Danish Technical Research Council under the Materials Research Programme.

References

[1] Needleman, A.: A continuum model for void nucleation by inclusion debonding, *J. App. Mech.* **54**:525-531, 1987.
[2] Hill, R.: A theory of the yielding and plastic flow of anisotropic metals, *Proc. Royal Soc. Lond.* **A193**:281-297, 1948.
[3] Barlat, F., Lege, D. J., Brem, J. C.: A six-component yield function for anisotropic materials, *Int. J. Plast.* **7**:693-712, 1991.
[4] Tvergaard, V.: Effect of fibre debonding in a whisker-reinforced metal, *Mat. Sci. & Eng.* **A125**:203-213, 1990.
[5] Tvergaard, V.: Effect of thickness inhomogeneities in internally pressurized elastic-plastic spherical shells, *J. Mech. Phys. S.* **24**:291-304, 1976.